

SUBSTORM TOPOLOGY IN THE IONOSPHERE AND MAGNETOSPHERE DURING A FLUX ROPE EVENT IN THE MAGNETOTAIL

O. Amm⁽¹⁾, R. Nakamura⁽²⁾, H.U. Frey⁽³⁾, Y. Ogawa⁽⁴⁾, M. Kubyskhina⁽⁵⁾, A. Balogh⁽⁶⁾, and H. Rème⁽⁷⁾

⁽¹⁾*Finnish Meteorological Institute, Space Physics Program, P.O. Box 503, FIN-00101 Helsinki, Finland
(Phone: +358 9 1929-4689; FAX: +358 9 1929-4603; Email: Olaf.Amm@fmi.fi)*

⁽²⁾*Space Research Institute, Austrian Academy of Sciences, Schmiedlstraße 6, 8042 Graz, Austria*

⁽³⁾*University of California, Space Sciences Laboratory, Centennial Drive at Grizzly Peak Boulevard, Berkeley, CA
94720-7450, USA*

⁽⁴⁾*Solar-Terrestrial Environment Laboratory, Nagoya University, Furo-cho, Chikusa-ku, Nagoya, 464-8601, Japan*

⁽⁵⁾*Institute of Physics, University of St. Petersburg, St. Petersburg 198904, Russia*

⁽⁶⁾*Imperial College London, Space & Atmospheric Physics Group, The Blackett Laboratory, Prince Consort Road,
London SW7 2BW, UK*

⁽⁷⁾*CESR/CNRS, 9, Avenue du Colonel Roche, 31028 Toulouse Cedex 4, France*

ABSTRACT

On August 13, 2002, at ~ 2300 UT, about 10 min after a substorm intensification, Cluster observes a flux rope in the central magnetotail, followed by a localised fast flow event about one minute later. Associated with the flux rope event, a traveling compression region (TCR) is seen by those Cluster spacecraft which reside in the lobe. In the conjugate ionospheric region in Northern Scandinavia, the MIRACLE network observes the ionospheric equivalent currents, and the electron densities and electric fields are measured by the EISCAT radar along a meridional scanning profile. Further, the auroral evolution is observed with the Wideband Imaging Camera (WIC) on the IMAGE satellite. We compare in detail the substorm evolution as observed in the ionosphere and in the magnetosphere, and examine whether topological correspondences to the flux rope event exist in the ionospheric signatures. The large-scale mapping of both the location and the direction of the flux rope to the ionosphere shows an excellent correspondence to a lens-shaped region of an auroral emission minimum. This region is bracketed by an auroral region equatorward of it which was pre-existing to the substorm intensification, and a substorm-related auroral region poleward of it. It is characterised by reduced ionospheric conductances with respect to its environment, and downward field-aligned current (FAC) observed both in the magnetosphere and in the ionosphere. As determined from the ionospheric data, this downward FAC area is moving eastward with a speed of ~ 2 km s⁻¹, in good agreement with the mapped plasma bulk velocity measured at the Cluster satellite closest to that area. Further southwestward to this leading downward FAC area, a trailing upward FAC area is observed that moves eastward with the same speed. The direction of the ionospheric electric field permits a current closure between these two FAC areas through the ionosphere. We speculate that these FAC areas may correspond to the ends of the flux rope in its symmetry direction.

1. INTRODUCTION

Helical magnetic field structures inside the magnetosphere have played an important role for the understanding of the process of magnetospheric

substorms since the early models of Schindler (1974) and Hones (1977), in which such structures, termed “plasmoids”, played a major role in transporting the substorm energy antisunwards. The minimum energy state of such helical magnetic field structures is represented by force-free magnetic flux ropes (Priest, 1990). These are elongated magnetic structures in the central axis of which the magnetic field is strongest and points along that axis. With increasing radial distance from that axis the field component along the axis direction diminishes, while the field component azimuthal to it increases. In a flux rope with cylindrical symmetry, no radial field with respect to the central axis exists. For a special class of flux ropes which can assumed to be force-free, the currents are flowing either in the direction of the magnetic field, or opposite to it. The magnetic field solutions for a force-free, cylindrical flux rope have been given by Lundquist (1950).

Tailward propagating plasmoids and flux ropes associated with them have been observed since the mid-1980's in the magnetotail's plasma sheet using data of the ISEE-3 satellite (e.g., Sibeck et al., 1984) and have later been extensively studied with Geotail data (e.g., Nagai et al., 1998; Ieda et al., 1998; Slavin et al., 1998). In addition to these tailward moving structures, also earthward moving flux ropes have been observed in the near tail ($X > \sim -30 R_E$; e.g., Moldwin and Hughes, 1994). Slavin et al. (2003) showed that these flux ropes are often closely associated with earthward bursty bulk flows (BBFs) in the plasma sheet of the magnetotail, i.e., high-speed plasma flows of several 100 km s⁻¹ (e.g., Baumjohann et al., 1990; Angelopoulos et al., 1992), and accordingly named them “BBF-type” flux ropes, in contrast to “plasmoid-type” flux ropes moving tailwards. Both types of flux ropes could in many cases reasonably be approximated by a force-free model.

While plasmoid-type flux ropes occur tailward of a major active reconnection X-line and therefore are not magnetically connected to the ionosphere, BBF-type flux ropes occur earthward of such an active reconnection X-line, and are thus at least embedded in an environment which magnetically maps to the ionosphere. The average properties of a BBF-type flux rope with respect to its magnetic field and plasma properties that a satellite encounters during the passage of such a structure have

been summarized in a superposed epoch analysis by Slavin et al. (2003): The $|B_y|$ component as well as the total magnetic field strength show a peak with a maximum excursion of the order of ~ 10 nT, and a total duration of the excursion of ~ 30 s. The B_z component simultaneously shows a dipolar structure with a first negative, then positive excursion (this behavior is opposite for plasmoid-type flux ropes). The difference between the opposite B_z peaks has the same order of magnitude as the $|B_y|$ peak. In addition, $|B_x|$ may also show a unipolar peak like $|B_y|$, which is interpreted as a sign of the orientation of the flux rope in the X-Y plane. In the statistical study of Slavin et al. (2003), this azimuthal orientation of a flux rope has been found to be quite variable. Further, an increase of the earthward plasma velocity has on average been observed ~ 40 s before the flux rope observation, and this velocity peaks at ~ 600 km s^{-1} within roughly a minute after the flux rope encounter. Ahead of the flux rope, collocated with the earthward flow increase, a compression region with increased ion densities has been observed. In the lobes neighboring to the flux rope, traveling compression regions (TCR) are formed due to the compression of the lobes by the “obstacle” flux rope and are co-moving with it (e.g., Slavin et al., 1984, 2005).

The question what features, if any, may topologically correspond to a BBF-type flux rope in the ionospheric evolution of a substorm has not yet been addressed. This question may in the first view look surprising, as a flux rope is ideally thought to be a closed magnetic structure and thus may not directly map magnetically to the ionosphere. Hence, we would like to stress that we do not claim any features seen in the ionosphere to be directly magnetically connected to the flux rope, but rather inspect whether any *topological* correspondences exist. Such topological relations may follow from the fact that the flux rope deforms the ambient magnetic field, causes compressions in front of it, inhibits plasma flow through it, etc. E.g., in this respect a TCR is a magnetospheric topological consequence of a flux rope caused by the deformation and compression of the lobe magnetic field lines due to its movement. However, we note that the solutions for a force-free cylindrical flux rope by Lundquist (1950) involve Bessel functions that extend to infinity, and there is no way to “cut” these solutions such that both the conditions of the flux rope being force-free and magnetically closed can be preserved. In the real case, the extension of the flux rope is limited at least by the extension of the magnetosphere. Hence, at one of the conditions mentioned will not be valid, particularly at the ends of the flux ropes seen along their major axis, which may allow current to flow in or out of the flux rope region.

In order to address the question posed above, in this paper we analyse Cluster satellite data, IMAGE WIC optical data, and conjugate MIRACLE and EISCAT ground-based data for a flux rope event observed by Cluster on August 13, 2002, at ~ 2259 UT.

2. INSTRUMENTATION AND OBSERVATIONS

During our our event on August 13, 2002, the Cluster satellite fleet (Escoubet et al., 2001) is situated in the northern near-Earth tail at $\sim X_{GSM} \sim -17 R_E$ in the

postmidnight sector (upper row). With $Z_{GSM} \sim -2.2 R_E$ Cluster 3 is situated by $\sim 0.4 - 0.6 R_E$ closer to the equatorial plane than the other three satellites, but takes a central position of the four spacecraft in the X- Y_{GSM} plane. The Cluster footprints in the northern ionosphere together with the ambient IMAGE ground magnetometer network stations (Viljanen and Häkkinen, 1997) are shown in Fig. 1 in the geographic coordinate system. They have been calculated with the Tsyganenko 89 magnetic field model (T89; Tsyganenko, 1989) under the prevailing value of $K_p=2$. The validity of the magnetic field modeling using the stated model and parameter has independently been confirmed with the Hybrid Input Algorithm model (Kubyskhina et al., 1999). The

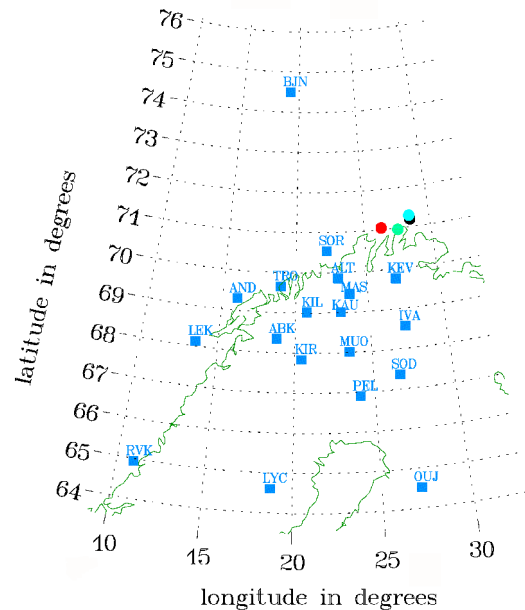


Fig. 1 Mapped positions of Cluster spacecraft to the ionosphere (dots, colours as in ?), and IMAGE magnetometer stations (squares with station abbreviations).

footprints are located above the northern coast of Scandinavia, close to the northeastern edge of the Scandinavian mainland IMAGE stations. Here and in the following, spacecraft 1 is marked with black colour, spacecraft 2 red, spacecraft 3 green, and spacecraft 4 blue.

From the different instruments onboard Cluster, for our study mostly data from the Fluxgate magnetometer (FGM, Balogh et al., 2001) and Cluster Ion Spectrometry (CIS, Rème et al., 2001) instruments are used. With respect to the CIS, data from the Hot Ion Analyser (HIA) are shown for spacecraft 1 and 4, while data from the Composition Distribution Function (CODIF) instrument have been used for spacecraft 3. Before the event, a plasma sheet thinning is observed starting from ~ 2230 UT. During this thinning, all Cluster spacecraft exit to the plasma sheet boundary layer (PSBL). Spacecraft 1, 2, and 4 later exit to the lobe, while spacecraft 3's position undulates between a PSBL-like and a lobe-like region. A weak electron injection onset is seen at one of the LANL

geostationary spacecraft at ~ 2250 UT (data not shown). After the event, a dipolarization and plasma sheet expansion takes place, and the spacecraft re-enter the plasma sheet, lead by spacecraft 3 at 2306 UT. During the following ~ 12 min after that re-entry, three distinct fast flow events take place with velocities in X_{GSM} direction up to ~ 1000 km s^{-1} (data not shown).

In this paper, we concentrate on the discussion and analysis of the magnetospheric and ionospheric observations in the immediate temporal vicinity of the flux rope event at ~ 2259 UT. A detailed plot of the Cluster data for a 6 min interval around that event is shown in Fig. 3 (next page). The flux rope event is bracketed by the two vertical dashed lines. The magnetic data shown have a 22 Hz resolution. The most pronounced feature in the magnetic data during that period is a positive peak in B_Y of ~ 9 nT in spacecraft 3, coincident with a bipolar signature of comparable amplitude in B_Z . This signature, with a first equatorward, then poleward B_Z component, corresponds to what is expected for a earthward moving or BBF-type flux rope as described in the introduction. Simultaneously with the B_Y increase, a sharp increase of B_X on top of a smoother decrease is measured at spacecraft 3. While the smooth decrease corresponds to a deeper entry of the spacecraft into the plasma sheet boundary layer, the sharp increase is interpreted as a tilt of the flux rope in the X-Y plane.

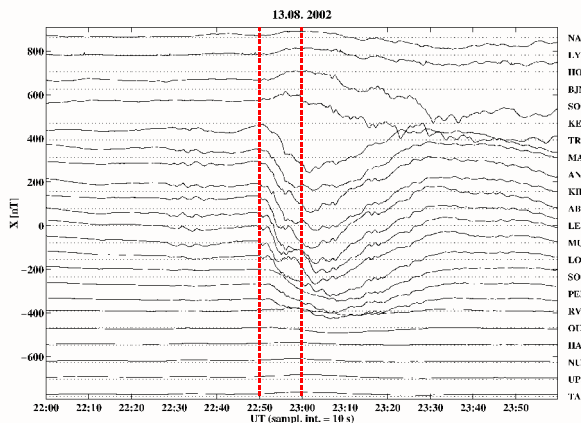


Fig. 2 Geographic north (X) component of IMAGE magnetograms on August 13, 2002, from 2200-0000 UT, in nT.

By comparison of the peak values in B_X and B_Y with respect to the background magnetic field, a tilt of $\sim 42^\circ$ in clockwise direction (if seen from $+Z$ direction) with respect to the Y axis is inferred. Also $|B|$ peaks during the flux rope, as expected (not shown in the Figure, but can indirectly be deduced from the peak in the magnetic pressure, bottom panel of Fig. 3). The duration of the B_Y and $|B|$ peaks lies with ~ 20 s well in the range of the statistical results of Slavin et al. (2003). Simultaneously with the flux rope, a downward field-aligned current (FAC) of ~ 3 nA m^{-2} is calculated using the curlometer technique (Dunlop et al., 2002; see fourth and fifth panel from the bottom in Fig. 3). Only a slight increase of the earthward flow velocity up to ~ 100 km s^{-1} is seen by Cluster 3 in association with the flux rope event. We interpret this fact such that due to the Cluster 3's location

in the PSBL, possibly existing faster and longer lasting flows in the central plasma sheet were not recorded.

The other three Cluster spacecraft (1, 2, and 4) which are located in the northern lobe encounter a traveling compression region (TCR), as can be seen from the increase in B_X and the dipolar B_Z signature which is smaller, but of similar orientation as the one of the flux rope in spacecraft 3. From the timing of the B_X peaks, the velocity of this magnetic signature has been inferred to ~ 1200 km s^{-1} in an earthward and eastward direction in the X-Y plane, tilted by $\sim 29^\circ$ clockwise from the $+X$ axis (if seen from $+Z$ direction). This value is well in accordance with the results of the TCR statistics by Slavin et al. (2005). As the direction of the core of the flux rope is expected to be roughly 90° tilted with respect to the motion of the associated TCR, this leads to an estimate for the flux rope tilt of $\sim 29^\circ$ clockwise from the $+Y$ axis (if seen from $+Z$ direction), which is somewhat smaller than the value of 42° deduced from the Cluster 3 data above. However, since Cluster 3 is located northward of the core of the flux rope, for the given geometry this increase of the apparent tilt angle with increasing distance from the core in $+Z$ direction is expected.

The X (geographic north) component of the IMAGE magnetometers are shown in Fig. 2 in a conventional magnetogram plot. Following a rather moderately disturbed period, the pre-existing westward electrojet intensifies at 2250 UT in all northern Scandinavian mainland stations (simultaneously with the observed electron injection at LANL; see first vertical dashed line in Fig. 2). The flux rope observation at Cluster occurs during the late expansion phase of the substorm as observed in IMAGE (see second vertical dashed line in Fig. 2). Note that some of the stations in the northeastern Scandinavian mainland, such as Masi (MAS) and Kevo (KEV), show a clear positive excursion which peaks at ~ 2300 UT. Subsequently, the recovery phase begins which lasts until ~ 2325 UT. The ground magnetic data will be analysed in more detail in the following section.

The Far Ultraviolet Wideband Imaging Camera (WIC) on the IMAGE satellite monitors the auroral emissions in the spectral range of 140-190 nm (Mende et al., 2000). On August 13, 2002, the field of view of the WIC covered almost the whole northern auroral region, with Northern Scandinavia located close to the limb of the observation area, and this limb shifting polewards during the time of interest around 2300 UT. Two major auroral regions are visible (data not shown): An equatorward, fainter, auroral structure is seen located at $\sim 68^\circ$ of latitude. This structure has been pre-existing before the substorm intensification at 2250 UT (data not shown). Starting from that substorm onset, a second, brighter auroral region has developed and moved polewards. At 2256:38 UT, this region peaks at $\sim 71.2^\circ$ latitude, while at 2300:43 UT, it has reached $\sim 72.7^\circ$ latitude at 16° longitude. To the west and to the east of Scandinavia, these two auroral regions appear to reunite, forming a convex lense-like shape. In the center of this lense, an area with clearly less auroral emission is observed, which at 2258:41 UT is located just at the northern coastline of Scandinavia. At 2300:43 UT, this area is again covered with moderate auroral emission,

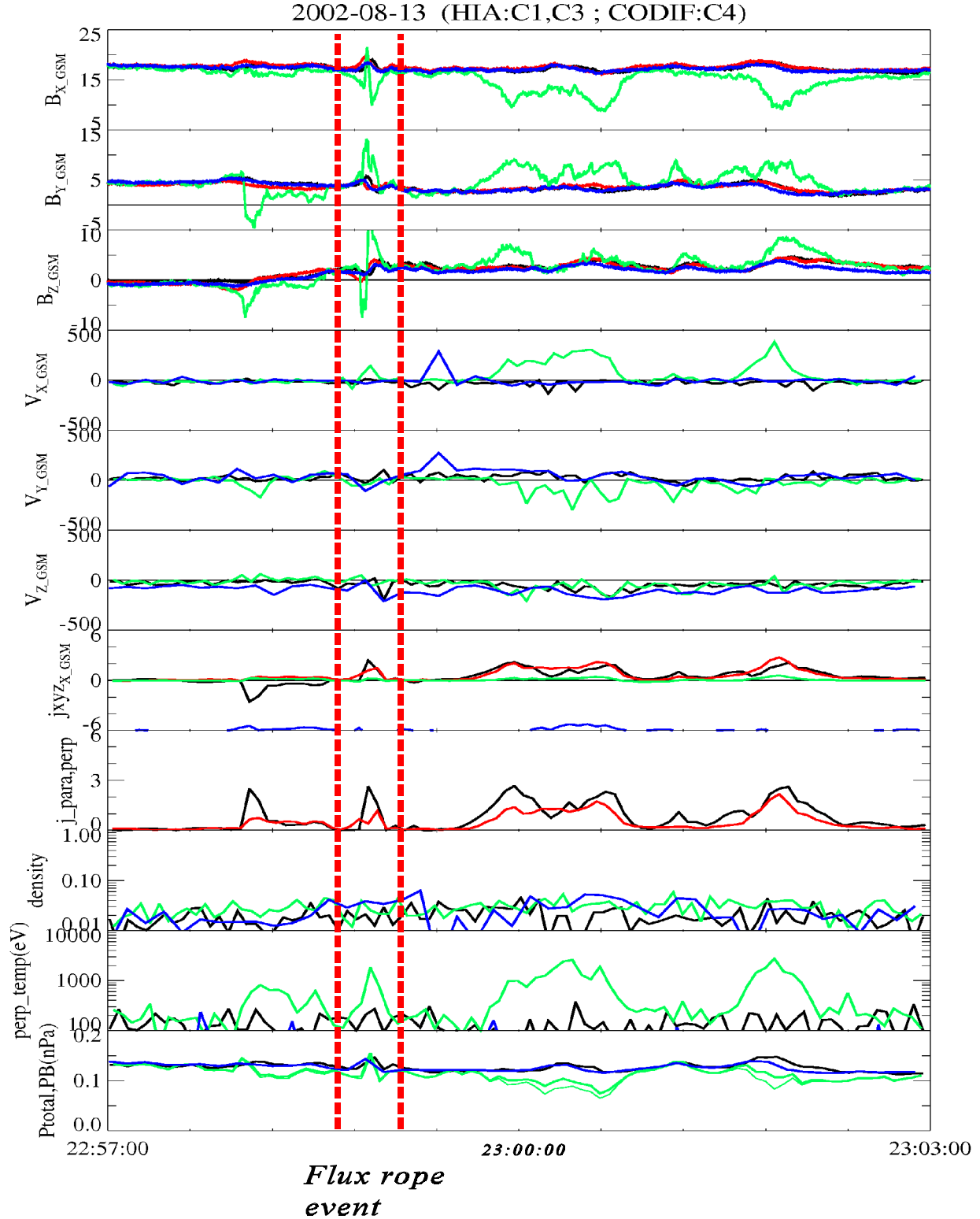


Fig. 3 Cluster FGM and CIS data of August 13, 2002, for the interval 2257-2303 UT. The CODIF instrument has been used for the CIS data of Cluster 4, HIA for CIS data of Cluster 1 and 3; colours for the different Cluster spacecraft as in Fig. 1. Panels from top to bottom: First to third panel: Magnetic field components in nT, in GSM coordinates; Fourth to sixth panel: Ion bulk velocities in km s^{-1} , in GSM coordinates; Seventh panel: Currents determined with the curlometer technique in nA m^{-2} , in GSM coordinates: black: X component, red: Y component, green: Z component; magenta: $\text{div } \vec{B}$ (quality parameter, should ideally be zero; plotted with an offset of -6 nA m^{-2} , for convenience); Eighth panel: Currents parallel (black) and perpendicular (red) to the magnetic field, in nA m^{-2} ; Ninth panel: Plasma density at the four different spacecraft, in cm^{-3} ; Tenth panel: Temperature perpendicular to the magnetic field, in eV; Eleventh panel: Total (thick line) and magnetic (thin line) pressure in nPa; the flux rope event is bracketed by the two vertical dashed lines.

while the “void” area may have traveled eastwards (however, this cannot be unambiguously concluded because of the border of the WIC field of view).

The European Incoherent Scatter Facility mainland radar (EISCAT; Folkestad et al., 1983) was operating in a beam-swinging mode during our event such that the main radar beam is moved equatorwards from 72.2° latitude to 67° latitude (at 117 km altitude) during 28 min, and then the antenna is directed back to the starting position within the following 2 min, in order to complete a full 30 min cycle. During our period of main interest, these cycles started at 2230 and 2300 UT, respectively. The main beam data are used to deduce, among others, the electron density, ion and electron temperatures, and ion velocity in the beam direction. By using all three EISCAT sites including the receiving stations at Kiruna and Sodankyla, also the full ion velocity vector in the F region (at 293 km altitude) and thus the electric field was derived.

3. ANALYSIS RESULTS AND DISCUSSION

The picture changes when we inspect the 2D distributions of the ionospheric quantities: Fig. 4 shows the WIC intensities over Northern Scandinavia together with the mapped location and direction of the flux rope, as well as the Cluster magnetic footprints. For the flux rope mapping, the blue line shows the estimate from the 90° rotated direction of the TCR motion, and the red line the estimate as determined from the Cluster 3 magnetic data. In both cases, for the mapping the estimated directions were linearly continued in the magnetospheric X-Y plane. The flux rope maps into the lens-shaped area of weak FUV emissions below 1000 R. Moreover, also the orientation of the mapped flux rope coincides well with that of the weak auroral emission region, which are both northeast-southwest aligned in the ionosphere. Note that although the 90° rotated direction of the TCR motion is expected to correspond best to the flux rope core direction, this conclusion is qualitatively not sensitive to the difference between the two estimates of the flux rope orientation. Since a flux rope effectively acts as an “obstacle” for particles precipitating from the tail to the ionosphere, it is likely that this signature is caused by an inhibition of such particles due to the presence of the flux rope.

A further topological correspondence to the flux rope is found in the 2D ionospheric current pattern. For that purpose, we calculate the 2D ionospheric equivalent currents $\vec{J}_{eq,ion}$ using the 2D SECS technique for the upward continuation of the ground magnetic field (Amm and Viljanen, 1999). Further, we decompose this currents according to $\vec{J}_{eq,ion} = \vec{J}_{df,ion} + \vec{J}_{lap,ion}$, where $\vec{J}_{lap,ion}$ is the part of the current which is divergence- and curl-free within our analysis area, while $\vec{J}_{df,ion}$ denotes the part of the current which is divergence-free, but not curl-free inside that area (e.g., Amm, 1997). (Note that $\vec{J}_{eq,ion}$ is by definition divergence-free, cf., e.g., Untiedt and Baumjohann, 1993). With such a decomposition, the main background westward electrojet will be contained in $\vec{J}_{lap,ion}$, while local features of the current system are seen in $\vec{J}_{df,ion}$. The evolution of this latter current system is shown in 1-min steps in Fig. 5, between 225650 and 225950 UT. Two oppositely directed current vortices are

visible, a clockwise one which is centered at $\sim 71.5^\circ$ latitude, and an anticlockwise one which is centered slightly poleward of 68° latitude. If the ionospheric conductances were uniform, the clockwise vortex would correspond to a downward FAC, and the anticlockwise one to an upward FAC. Both vortices are moving synchronously eastward, with a speed of $\sim 2 \text{ km s}^{-1}$. The poleward vortex is reaching the Cluster satellites just at the time when a downward FAC is also observed in the Cluster data (cf lower right panel in Fig. 5 and Fig. 3b). Comparing the location of the two vortices at 225850 UT with the FUV image which was taken 10 s earlier (Fig. 4), it can be seen that the anticlockwise vortex is well collocated with the lens-shaped emission minimum, while the clockwise vortex is well collocated with the emission maximum around 68.5° latitude, which supports the interpretation of the current vortices as downward and upward FAC regions, respectively. We notice that the tilt of the axis between the two current vortices is comparable with the tilt of the ionospheric projection of the flux rope direction (the two estimates are marked by the blue and red lines in the 225950 UT panel of Fig. 5, similarly to Fig. 4). Furthermore, with $\sim 2.4 \text{ km s}^{-1}$, the mapped eastward bulk velocity observed at Cluster 4 (which is located closest to the central latitude of the anticlockwise vortex) agrees well with the eastward speed of the current vortices.

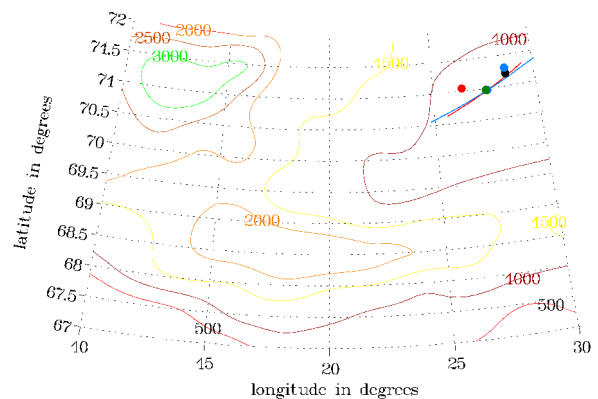


Fig. 4 Cluster footprints (dots, colours as in ?), and direction estimates of the flux rope as mapped to the ionosphere (blue line: based on 90° rotated TCR direction of motion; red line: based on the orientation measured by Cluster 3; in both cases linearly continued in the magnetospheric X-Y plane) at 2259:50UT, together with WIC emissions in R at 2258:41 UT (iso contour lines).

Thus we conclude that in a 2D view, there are several clear topological ionospheric correspondences to the flux rope event: A lens-shaped decrease of the ionospheric FUV emissions which is collocated with a downward FAC area that moves eastward with a speed close to the bulk velocity of the plasma as measured in the magnetosphere. This leading downward FAC area is balanced by a trailing upward FAC area which moves eastward at the same speed at lower latitudes. On the other hand, no ionospheric topological correspondence is found to the mentioned fast eastward motion of the B_x peaks of the TCR, which would map to a $\sim 22 \text{ km s}^{-1}$

eastward velocity component in the ionosphere.

A tentative interpretation of the topological correspondence might be that the two current vortices in $\vec{J}_{df,ion}$ are the “edges” of a flux rope in its symmetry direction where part of the current flowing in its central area is diverted into upward and downward FAC, respectively. Both in the ionosphere and in the flux rope (where $\vec{j} \parallel \vec{B}$), the currents are flowing southwestwards. (Note that the $\vec{J}_{df,ion}$ currents in Fig. 5 would in case of uniform conductances correspond to Hall currents, but the total currents related to the double vortex structure are expected to flow from the downward FAC area in the northeast to the upward FAC area in the southwest. This is also discussed below when looking at the ionospheric electric field.) For the flux rope, this current direction also corresponds to the prevailing positive IMF B_Y component (data not shown). Hence, in this interpretation there is no current circuit between ends of the flux rope and the ionosphere, since in this case the current direction in both domains should be opposite, and such a circuit would miss a current generator. Rather, the current generated further tailward in the magnetosphere could close either via the ionosphere, or close by “tunneling” through the flux rope, in the same direction. If this interpretation is correct, the role of the flux rope in this picture should depend on the B_Y component prevailing in it, since only for a positive B_Y the currents could be closed in the direction as required during a substorm. We emphasize that this interpretation

is at the present stage speculative, and more work needs to be done to either verify or falsify it. However, it would be consistent with the topology of the horizontal currents and FAC, as observed by Cluster and in the ionosphere.

In order to inspect whether or not the two FAC regions can be connected by ionospheric currents, the electric field observations by EISCAT are shown in a superposed vector plot in Fig. 6. The measurements of the 2230-2300 UT scan are shown at their actual observation points, while measurements of later scans have been shifted eastward in space, and those of earlier scans westwards. Again, the observation times are indicated at the vectors. We note that before and later equatorward of the substorm region, large southeastward pointing electric field vectors with magnitudes partly well above 100 mV m^{-1} are seen. This high electric field region, which is independently also confirmed by a comoving area of enhanced ion temperatures (data not shown), moves equatorward with a speed of $\sim 0.1 \text{ km s}^{-1}$. However, as this interesting feature is pre-existing to the substorm, its detailed analysis lies outside the scope of this paper. We concentrate on the electric field structure after the activation and inside the substorm area (i.e., poleward of $\sim 68^\circ$ latitude) which is marked by the red box in Fig. 6. Especially during the 2300-2330 UT scan, the electric field magnitudes are depressed to values of $20\text{-}30 \text{ mV m}^{-1}$, as to be expected due to the conductance enhancement during the substorm. During this first scan, the electric field points mostly southward, which is just

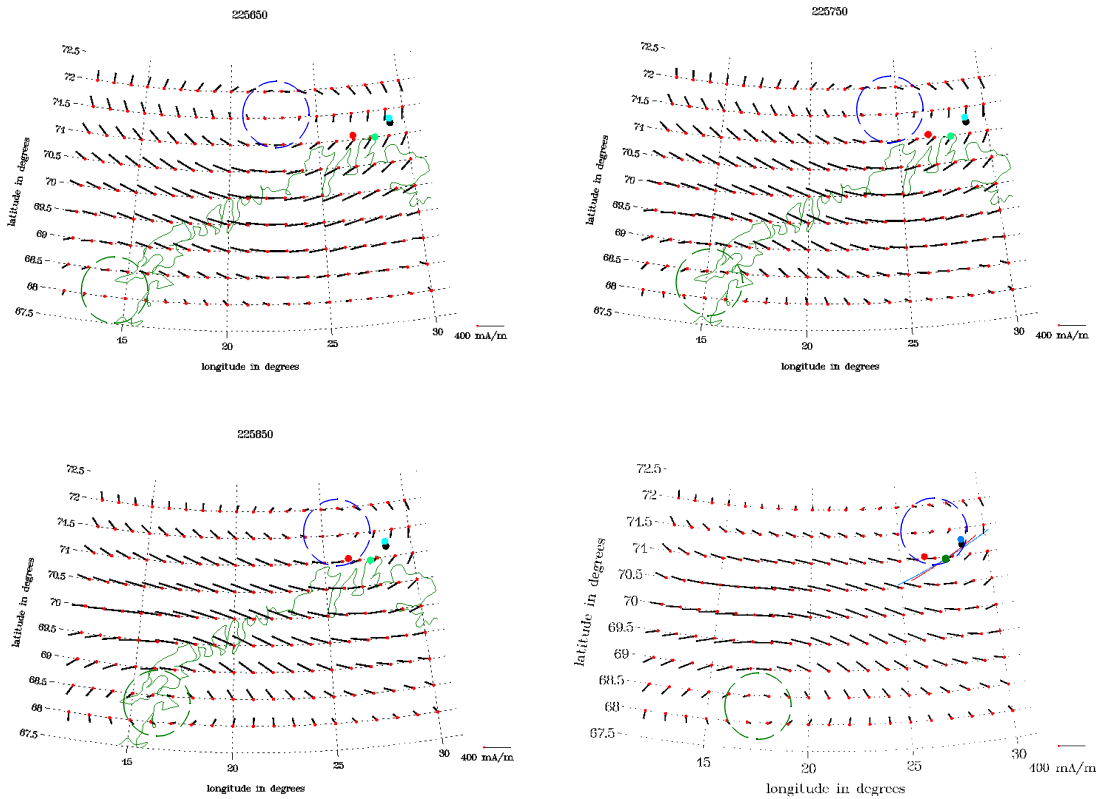


Fig. 5 Evolution of divergence-free equivalent currents (only part which has curls in the analysis area) between 2256:50-2259:50 UT, and Cluster magnetic footprints (colours like in Fig. 1). Blue and green dashed circles mark the location of clockwise and anticlockwise current vortices, respectively. Mapped flux rope directions as in Fig. 4.

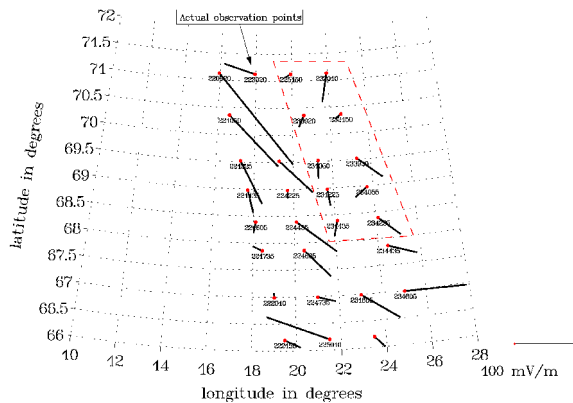


Fig. 6 Electric field measured by EISCAT for four consecutive scans from north to south between 2200-0000 UT (two vectors have been deleted for data quality reasons). Data of the scan 2230-2300 UT are shown at the actual observation points, data of earlier scans are shifted westward, of later scans eastward. The area enclosed by the red dashed line marks the spatio-temporal domain of the substorm intensification and recovery phase.

the electric field direction required to direct the total horizontal ionospheric current into a west-southwestward direction, in good correspondence with the direction between the downward and upward FAC regions in Fig. 5. During the 2330-0000 UT scan, i.e., already at the end and after the recovery phase of the substorm, the electric field magnitudes somewhat increase again and the directions become more variable. Hence we conclude that the EISCAT electric field data during the substorm event is compatible with the current structure found from the magnetic field data, and thus further confirms our interpretation of the two current vortices as oppositely directed FAC regions.

4. SUMMARY AND CONCLUSIONS

During the expansion phase of a substorm on August 13, 2002, around 2259:50 UT Cluster 3 observed an earthward traveling BBF-type flux rope in the PSBL, while the other three Cluster spacecraft experienced the signature of a TCR in the northern lobe. Our search for possible topological correspondences in the conjugate ionosphere to these magnetospheric substorm features has yielded the following results:

- At the ionospheric footprint of the flux rope, a convex lens-shaped FUV emission minimum region is observed inside which the ionospheric conductances are diminished with respect to the environment. The alignment of the lens shape corresponds well to the mapped direction of the flux rope.
- This FUV emission minimum region is collocated with a downward FAC area as both measured with Cluster and inferred from the ground-based data. The downward FAC area is moving eastward with a speed of $\sim 2 \text{ km s}^{-1}$ which is in good agreement with the mapped bulk velocity measured at the Cluster spacecraft closest to that area.
- Comoving with this leading downward FAC area at $\sim 71.5^\circ$ latitude is a trailing upward FAC area

slightly poleward of 68° latitude. The tilt angle between these two FAC areas is in good agreement with the tilt angle of the flux rope mapped to the ionosphere. The electric field in the region is consistent with a current flow from the downward to the upward FAC area in southwestward direction. This is the same direction in which the current in the flux rope is flowing if it is assumed to be close to force-free.

- No ionospheric topological correspondence can be found to the fast ($\sim 1200 \text{ km s}^{-1}$) earthward movement of the B_x peaks in the magnetosphere related to the TCR.

We suggest a possible interpretation of these topological correspondences as follows: The two FAC regions of opposite polarity may correspond to the ends of the flux rope in the direction of its central axis, where the magnetic topology is not closed and current can partly be diverted into FAC (or vice versa). If this hypothesis applies, it would mean that the current generated further downtail in the magnetosphere can either close via the ionosphere, or “tunnel” through the flux rope in the same direction. Such a current closure during a substorm would only be possible if the core magnetic field in the flux rope points westwards, i.e., in +Y direction like in our case. We emphasize that at the present stage this interpretation is a hypothesis, and more work needs to be done in order to either verify or falsify it. However, the interpretation appears to be consistent with the magnetospheric and ionospheric data and analysis presented in this study.

ACKNOWLEDGMENTS

The authors would like to thank James Slavin for valuable discussions. We are indebted to the director and staff of EISCAT for operating the facility and supplying the data. EISCAT is an International Association supported by Finland (SA), France (CNRS), Germany (MPG), Japan (NIPR), Norway (NFR), Sweden (NFR) and the United Kingdom (PPARC).

REFERENCES

- Amm, O., and Viljanen, A.: Ionospheric disturbance magnetic field continuation from the ground to the ionosphere using spherical elementary current systems, *Earth, Planets and Space*, 51, 431, 1999.
- Amm, O.: Ionospheric elementary current systems in spherical coordinates and their application, *J. Geomagn. Geoelectr.*, 49, 947, 1997.
- Angelopoulos, V., Baumjohann, W., Kennel, C.F., Coroniti, F.V., Kivelson, M.G., Pellat, R.J., Walker, R.J., Lühr, H., and Paschmann, G.: Bursty bulk flows in the inner central plasma sheet, *J. Geophys. Res.*, 97, 4027, 1992.
- Balogh, A., Carr, C.M., Acuña, M.H., Dunlop, M.W., Beek, T.J., Brown, P., Fornaçon, K.H., Georgescu, E., Glassmeier, K.-H., Harris, J., Musmann, G., Oddy, T., and Schwingenschuh K.: The Cluster Magnetic Field Investigation: overview of in-flight performance and initial results, *Annales Geophysicae*, 19, 1207-1217, 2001.
- Baumjohann, W., Paschmann, G., and Lühr, H.: Characteristics of high speed ion flows in the plasma

- sheet, *J. Geophys. Res.*, 95, 3801, 1990.
- Dunlop, M. W., Balogh, A., Glassmeier, K.-H., and Robert, P.: Four-point Cluster application of magnetic field analysis tools: The Curlometer, *J. Geophys. Res.*, 107(A11), 1384, doi:10.1029/2001JA005088, 2002.
- Escoubet, C. P., Fehringer, M., and Goldstein, M.: The Cluster mission, *Ann. Geophysicae*, 19, 1197-1200, 2001.
- Folkestad, K., Hagfors, T. und Westerlund, S.: EISCAT: An updated description of technical characteristics, *Radio Sci.*, 18, 867, 1983.
- Hones, E.W., Jr.: Substorm processes in the magnetotail: Comments on "On hot tenous plasma, fireballs, and boundary layers in the Earth's magneotail" by L.A. Frank et al., *J. Geophys. Res.*, 82, 5633, 1977.
- Ieda, A., Machida, S., Mukai, T., Saito, Y., Yamamoto, T., Nishida, A., Terasawa, T., and Kokubun, S.: Statistical analysis of plasmoid evolution with GEOTAIL observations, *J. Geophys. Res.*, 103, 4435, 1998.
- Kubyschkina, M.V., Sergeev, V.A., and Pulkkinen, T.I.: Hybrid Input Algorithm: An event-oriented magnetospheric model, *J. Geophys. Res.*, 104, 24977, 1999.
- Lundquist, S.: Magnetohydrostatic fields, *Ark. Fys.*, 2, 361, 1950.
- Mende, S.B., Heeterds, H., Frey, H.U., Lampton, M., Geller, S.P., Abiad, R., Siegmund, O., Tremsin, A.S., Spann, J., Dougani, H., Fuselier, S.A., Magoncelli, A.L., Bumala, M.B., Murphree, S., and Trondsen, T.: Far ultraviolet imaging from the IMAGE spacecraft: 2. Wideband FUV imaging, *Space Sci. Rev.*, 91, 271, 2000.
- Moldwin, M.B., and Hughes, W.J.: Observations of earthward and tailward propagating flux rope plasmoids: Expanding the plasmoid model of geomagnetic substorms, *J. Geophys. Res.*, 99, 184, 1994.
- Nagai, T., Fujimoto, M., Saito, Y., Machida, S., Terasawa, T., Nakamura, R., Yamamoto, T., Mukai, T., Nishida, A., and Kokubun, S.: Structure and dynamics of magnetic reconnection for substorm onsets with GEOTAIL observations, *J. Geophys. Res.*, 103, 4419, 1998.
- Priest, E.R.: The equilibrium of magnetic flux ropes, *Geophys. Monogr.*, 58, 1, 1990.
- Rème, H., Aoustin, C., Bosqued, J.M., Dandouras, I., B. Lavraud, B., Sauvaud, J.A., Barthe, A., Bouyssou, J., Camus, Th., Coeur-Joly, O., Cros, A., Cuvilo, J., Ducay, F., Garbarowitz, Y., Medale, J. L., Penou, E., Perrier, H., Romefort, D., Rouzaud, J., Vallat, C., Alcaydé, D., Jacquey, C., Mazelle, C., d'Uston, C., Möbius, E., Kistler, L. M., Crocker, K., Granoff, M., Mouikis, C., Popecki, M., Vosbury, M., Klecker, B., Hovestadt, D., Kucharek, H., Kuenneth, E., Paschmann, G., Scholer, M., Sckopke, N., Seidenschwang, E., Carlson, C. W., Curtis, D.W., Ingraham, C., Lin, R. P., McFadden, J. P., Parks, G. K., Phan, T., Formisano, V., Amata, E., Bavassano-Cattaneo, M.B., Baldetti, P., Bruno, R., Chionchio, G., Di Lellis, A., Marcucci, M.F., Pallochia, G., Korth, A., Daly, P.W., Graeve, B., Rosenbauer, H., Vasyliunas, V., McCarthy, M., Wilber, M., Eliasson, L., Lundin, R., Olsen, S., Shelley, E.G., Fuselier, S., Ghielmetti, A.G., Lennartsson, Escoubet, C.P., Balsiger, H., Friedel, R., Cao, J.-B., Kovrazhkin, R.A., Papamastorakis, I., Pellat, R., Scudder, J., and Sonnerup, B.: First multispacecraft ion measurements in and near the Earth's magnetosphere with the identical Cluster ion spectrometry (CIS) experiment, *Annales Geophysicae*, 19, 1303-1354, 2001.
- Schindler, K.: A theory of the substorm mechanism, *J. Geophys. Res.*, 79, 2803, 1974.
- Sibeck, D.G., Siscoe, G.L., Slavin, J.A., Smith, E.J., Bame, S.J., and Scarf, L.: Magnetotail flux ropes, *Geophys. Res. Lett.*, 11, 1090, 1984.
- Slavin, J.A., Fairfield, D. H., Kuznetsova, M. M., Owen, C. J., Lepping, R. P., Taguchi, S., Mukai, T., Saito, Y., Yamamoto, T., Kokubun, S., Lui, A. T. Y., and Reeves, G. D.: ISTP observations of plasmoid ejection: IMP 8 and Geotail, *J. Geophys. Res.*, 103, 119, 1998.
- Slavin, J.A., Lepping, R.P., Gjerloev, J., Fairfield, D.H., Hesse, M., Owen, C.J., Moldwin, M.B., Nagai, T., Ieda, A., and Mukai, T.: Geotail observations of magnetic flux ropes in the plasma sheet, *J. Geophys. Res.*, 108, 1015, doi:10.1029/2002JA009557, 2003.
- Slavin, J.A., Smith, E.J., Tsurutani, B.T., Sibeck, D.G., Singer, H.J., Baker, D.N., Gosling, J.T., Hones, E.W., and Scarf, F.L.: Substorm associated traveling compression regions in the distant tail: ISEE-3 geotail observations, *Geophys. Res. Lett.*, 11, 657, 1984.
- Slavin, J.A., Tanskanen, E., Hesse, M., Owen, C.J., Dunlop, M.W., Imber, S., Lucek, E., Balogh, A., and Glassmeier, K.-H.: Cluster observations of traveling compression regions in the near tail, *J. Geophys. Res.*, 110, A06207, doi:10.1029/2004JA010878, 2005.
- Tsyganenko, N.A.: A magnetospheric field model with a warped tail current sheet, *Planet. Space Sci.*, 37, 5, 1989.
- Untiedt, J., and Baumjohann, W.: Studies of polar current systems using the IMS Scandinavian magnetometer array, *Space Sci. Rev.*, 63, 245, 1993.
- Viljanen, A., and Häkkinen, L.: IMAGE magnetometer network, in: *Satellite-Ground Based Coordination Sourcebook* (eds. M. Lockwood, M.N. Wild and H.J. Opgenoorth). ESA publications SP-1198, p. 111ff., 1997.